International Journal of Control, Automation and Systems 15(1) (2017) 16-24
http://dx.doi.org/10.1007/s12555-016-0470-3
ISSN:1598-6446 eISSN:2005-4092
http://www.springer.com/12555

Design of an Optical Soft Sensor for Measuring Fingertip Force and Contact Recognition

Haedo Cho, Hyosang Lee, Yeongjin Kim, and Jung Kim*

Abstract: Among the various ways to estimate user intention in hand exoskeletons, a contact force measurement is definitely the most straightforward and intuitive method. A force sensor, located at the center of a fingertip usually, hinders the tactile sensation of the user by blocking the contact between an object and the fingertip. To overcome this problem, a soft force sensor with horse shoe shape is utilized to measure the contact force and provide the tactile sensation to the user. This work presents the mechanical design, implementation and evaluation of a soft fingertip force sensor. To maximize tactile sensation of the user, we adopted a horse shoe shape structure to leave the finger pad exposed. An optical sensing mechanism was selected for its relatively fast response compared to other soft sensors. The whole sensor system has a soft exterior providing flexibility and a user-friendly interface. To evaluate the sensor's performance, we carried out sensor optimization process and calibration experiment with a customized test bed. Then, we investigated both static and dynamic response and observed the mechanical behavior and light intensity changes caused by the cross sectional shape and base/agent ratio of PDMS. Lastly, we applied the proposed sensor to the glove type fingertip force monitoring system. The sensor estimates the index finger tip force with high accuracy ($R^2 = 0.96$) within $5N$ range.

Keywords: Flexible sensor, force sensor, hand exoskeleton, open finger pad structure, optical sensor.

1. INTRODUCTION

Loss of muscle strength is closely interlinked with lowering health-related quality of life, and in particular grip strength plays an important role in performing wide range of activities for daily living (ADL) [1, 2]. The reasons for losing grip strength are aging [3], reduced muscle mass [4], rheumatoid arthritis [5], and most of all, the effect of imperfect recovery from stroke and spinal cord injury resulting in permanent or temporary weakness in grip strength [6, 7]. People who have an occupation requiring repetitive and large grip force are very likely to suffer work-related musculoskeletal disorders(WMSDs) [8]. Assistive hand exoskeletons can support people suffering from weakened grip strength by providing additional force. The classification of the various types of assistive hand exoskeletons depends on how the wearer's intention is examined: finger pad contact force [9–11], finger motion [12–14], surface electromyography (sEMG) [15, 16]. The measurement of finger pad contact force is the simplest and the most intuitive method amongst the rest. Measuring contact force does not involve any signal cross talk between fingers or rely on skin conditions - despite its significance in utilizing sEMG signal. In addition, it can be applied to both isometric and isokinetic conditions. However, the wearers lose their tactile sensation in manipulating objects since the force sensor is located at the center of the fingertip. The tactile sensation has a primary role in dexterous manipulation and it prevents excessive gripping force or slipping [17]. To achieve force measurement and wearer's tactile sensation simultaneously, there were several researches related to indirect force measurement; employing the lateral deformation of finger pad [18, 19] and the change of fingernail color [20]. These methods do not obstruct the tactile sensation but disturb natural grip motion and require a bespoke for every host because they are made of rigid material.

Recent interests in applying soft materials to wearable robotics have arisen thanks to their compliance, impact resistance, reduced-cost and suitability for measurements on complex shape such as the human body [21–24]. Having high compliance and flexibility, soft sensors produce

Manuscript received August 1, 2016; revised October 27, 2016; accepted October 29, 2016. Recommended by Guest Editor Sungwan Kim. This research was supported by Basic Science Research Program through the National Research Foundation of Korea (NRF) funded by the Ministry of Education (2015R1A2A2A01002966). The authors are grateful to James Kinch and Daniel Gutierrez from University of Leeds for their enthusiastic discussion and help. In addition, we thank to Seeun Im from McGill university for her technical support in writing.

Haedo Cho, Hyosang Lee, and Jung Kim are with Department of Mechanical Engineering, Korea Advanced Institute of Science and Technology, 291 Daehak-ro, Yuseong-gu, Daejeon 34141, Korea (e-mails: johncho@kaist.ac.kr, ginogino@kaist.ac.kr, jungkim@kaist.ac.kr). Youngjin Kim is with Department of Mechanical Engineering, Incheon National University, 8-204, 119 Academy-ro, Yeonsu-gu, Incheon, 22012, Korea (e-mail:Ykim@inu.ac.kr).
* Corresponding author.

©ICROS, KIEE and Springer 2016

physical movement information from a host with minimal interference. Motion sensing with soft sensors such as artificial skin show good wearability and mobility [23, 24]. Soft sensors are catergorized into pieresistive [25, 26], piezoelectric [27, 28], capacitive [29] and optical type [30–32]. In general, optical sensors have certain advantages that include: immunity to electro magnetic interference (EMI), small size and signal light transmission capability [33]. Most of all, polymer waveguide can give good compliance to object curvature as well as being highly adaptable to modulation in sensor feature [32].

In this paper, we present a soft sensor that measures the fingertip force and provides the tactile sensation simultaneously. The sensor consists of a polymer waveguide allowing a fully soft sensing component. The sensing method in this work is inspired by the polymer optical fiber based stretchable sensor that measures pressure, strain and curvature [32]. To utilize it as a pressure sensor only and optimize for a force measurement, we adopted the horse shoe shape leaving the finger pad exposed. This prevents obstruction of tactile sensation for the user. The paper is organized as follows: In Section 2, we discuss the sensor principle, fabrication, and experimental setup followed by the design optimization in Section 3. Sensor characterziation is discussed in Section 4. In Section 5, we describe fingertip force estimation experiment. Finally, we make some concluding remarks in Section 6.

2. CONCEPT AND DESIGN

The overview of the sensor system is shown in Fig. 1. To measure the fingertip force and leave the finger pad exposed for tactile sensation, the sensor is to be designed and located as Fig. 1. shows. The wearer wore the glove with putting some red ink on the finger pad. Fig. 1. shows the result of gripping a cylindrical object with the white paper on it. The area of fingerprint proves that the wide contact between finger and object was achieved.

Fig. 1. Open finger pad force monitoring glove.

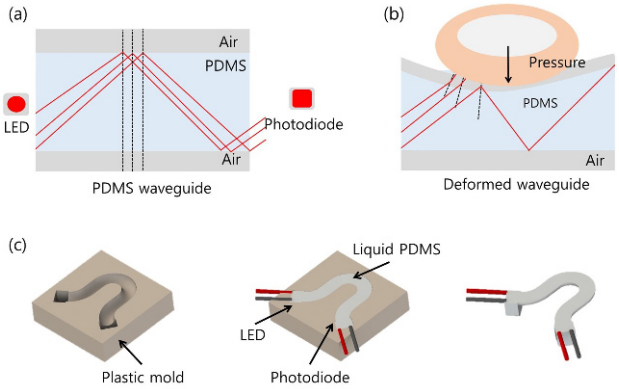

Fig. 2. (a), (b) The schematic of sensing principle. (c) The process of fabrication.

2.1. Sensing principle

In a polymer waveguide, the intensity of light can be modulated corresponding to the deformation of the structure, called light intensity modulation [30]. Fig. 2. shows a schematic of the working principle of PDMS based optical pressure sensor. As the intensity of light transmitted by the optical fiber is proportional to a number of modes, a deformation of the optical fiber itself leads to the modulation of the light intensity. In this work, we selected PDMS as an optical waveguide since its mechanical and optical properties are well characterized. It has a high transparency and a low attenuation level (approximately 0.4 dB/cm). Furthermore, it is nontoxic, biocompatible with human skin, thus, well-suited for using in biomedical area [34]. As PDMS waveguide (refractive index= 1.4225@632.8 nm) is surrounded by air (refractive index= 1), a number of mode can be guided inside of the core. The deformation of the PDMS waveguide surface by an applied pressure changes of modes inside the PDMS waveguide. As the surface is deformed, modes of light below the critical angle pass through cladding layer and fewer number of waveguide modes will be detected (see Fig. 2(b)). This leads to optical loss and causes a decrease of the guided light intensity.

2.2. Fabrication process and sensor design

Fig. 2(c) shows the process of fabrication. PDMS polymer was used for the waveguide in order to make the transparent and soft elastomer. Then, we attached a red light-emitting diode (CREE XLamp XBD) and photodiode (Everlight CLS15) at the ends of the mold, respectively. The

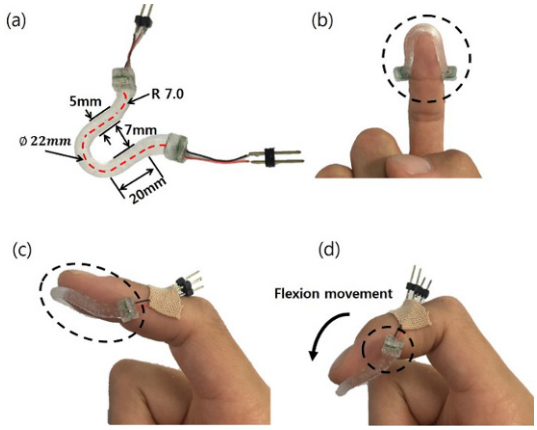

Fig. 3. Prototype (a) Sensor dimension (b) The finger pad is fully exposed (c) Minimizing interference of the sensor in touch motion (d) Minimizing the effect of bending of the sensor.

reason for selecting a red light LED (light-emitting diode) is that it features high responsivity (the electrical output per optical input) among commercialized LED. After having fully poured liquid PDMS into the mold, we put it in the oven for 2 hours at 70°C. Fig. 3. shows the prototype of the sensor. The dimension of the sensor is shown in Fig. 3(a). The total length of the sensor was determined to cover only distal phalange part of the finger. This leads to minimize the bending effect in flexion movement. Furthermore, we added another curvature at the end of the sensor to avoid the interference in touch motion.

2.3. Experimental setup

The sensors response to cyclic pressure was tested by the motorized test bed as shown in Fig. 4(a). The output signal was the voltage value from the photodiode. A strain gauge type load cell (651 AL, KTOYO Co., Ltd., Uijeongbu, Korea) was used to measure the reference force data. Fig. 4(b) reprensents a schematic of eletronic circuits of optical components and data acqusition system. When the photodiode receives light energy, it converts light energy into a current because of its photoelectric effect. To measure the current produced, we attached a resistor in parallel and measured the voltage signal via the data acquisition system (Q8-USB, Quanser, USA). To surpress the noise during supplying power to the LED, the combination of the capacities is applied as shown in Fig. 4(b).

3. SENSOR DESIGN OPTIMIZATION

There are many parameters affecting the performance of the sensor. We observed the effect of two parameters: the base/agent ratio of PDMS and the cross sectional shape. We inspected the quantified hysteresis level and linearity relative to linear approximation and sensivitiy.

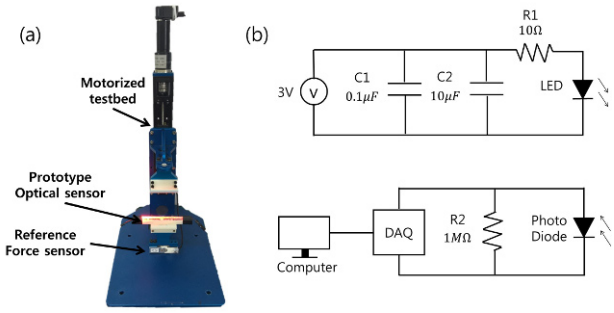

Fig. 4. (a) Motorized test bed with a reference strain-gauge type load cell (b) The electronic circuits of the optical components and hardware configuration.

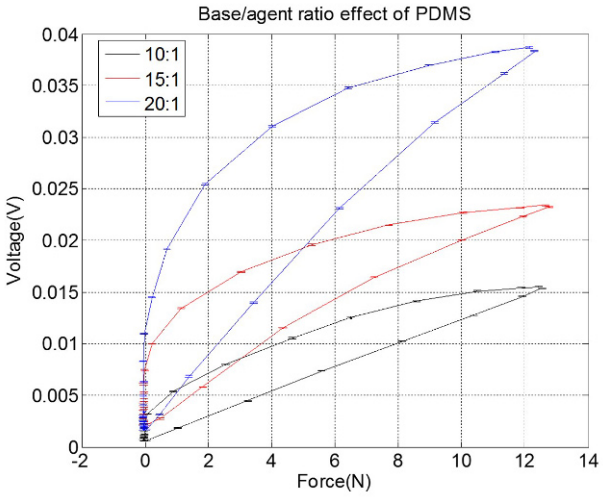

Fig. 5. Force-Voltage profile of the sensors with three different base/agent ratio. Note: Lower base/agent ratio means larger stiffness.

3.1. Base/agent ratio

Fig. 5. shows 20 cycles of the hystersis behavior of different base/agent ratio. Base/agent ratio affects stiffness of the PDMS based pressure sensor. Lower base/agent ratio means larger stiffness (smaller deformation under same loading condition). Less hysteresis behavior was observed at the sensor with the lowest base/agent ratio. This result implies that the change of the optical sensor voltage output mainly depends on a structure change (deformation) of the sensor. When the sensor is loaded, the voltage change of the proposed sensor matches the force profile of the reference sensor well ($R^2 = 0.99$). While unloading, the polymer waveguide takes time to restore its original structure because of its viscoelastic characteristic of the PDMS material material. This is the main reason for the slightly increased discrepancy between the signal in loading and unloading condition as the loading rate increased.

In terms of the base offset, the lowest value was ob-

Table 1. Sensor features according to base/agent ratio of PDMS.

Base/agent ratio	Sensitivity (V/N)	Linearity R^2	Offset (V)	Max std(V)
10:1	0.0012	0.9985	0.0005	6.09×10^{-5}
15:1	0.0017	0.9871	0.0021	1.05×10^{-4}
20:1	0.0031	0.9928	0.0016	7.4×10^{-5}

served at the sensor with the lowest base/agent ratio. This is because the sensor structure undergoes residual strain after load is applied [35]. The stiffer structure shows less baseline offset since it has less time delay and less viscoplastic behavior. When it comes to sensitivity, the highest base/agent ratio shows the highest sensitivity value under the same loading condition. This result coincides with the mechanical property of the PDMS structure. When we apply the same force on the sensors, the lowest strain is induced at the sensor with the highest stiffness. In this paper, we selected 10:1 as base/agent ratio because it shows the lowest hysteresis, offset and high flexibility as a soft sensor.

3.2. Cross sectional shape

Two different cross sectional shapes, rectangular one and semicircle one, of the sensors were tested. As shown in Fig. 6(a), each of them has the identical width of 5mm, and thickness of 2.5 mm. Both of the sensors were applied by a force loading from 0 to 12 N with 0.5 Hz sinusoidal loading profile. Fig. 6(b) shows the results of the sensitivity and linearity of each sensor. The sensitivity of the rectangular shape sensor was 0.0026 and the semi-circle shape one was 0.0037. Under the same loading condition, the sensitivity value of the semicircle sensor is 1.32 times higher than the rectangular shape. Because the deformation per unit force is more induced at the smaller contact area, the higher sensitivity was observed in the semicircle shape sensor. In this paper, we adopted the semicircle shape sensor as it shows better performance in terms of sensitivity.

4. STATIC AND DYNAMIC CHARACTERIZTION

4.1. Static test: step response

We tested the step response of the semicircle sensor to determine the response time. We set up the amount of displacement of the motorized test bed as 0.3 mm. The time constant of the sensor was 33 ms, and 90 % of the time constant for our sensor turned out to be 258 ms as shown in Fig. 7. This result is similar to the response time of the previously reported optical pressure sensor [30]. The response of the optical sensor is mainly governed by the mechanical behavior of the PDMS substrate because the light propagation and detection are as highly rapid as less than milliseconds.

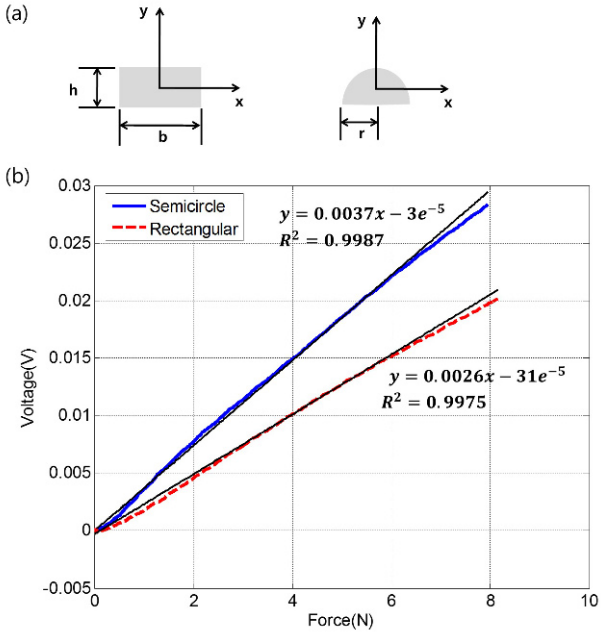

Fig. 6. Reference force to Voltage graph according to the cross sections of the sensors (a) Semicircle shape one (b) Rectangular shape one.

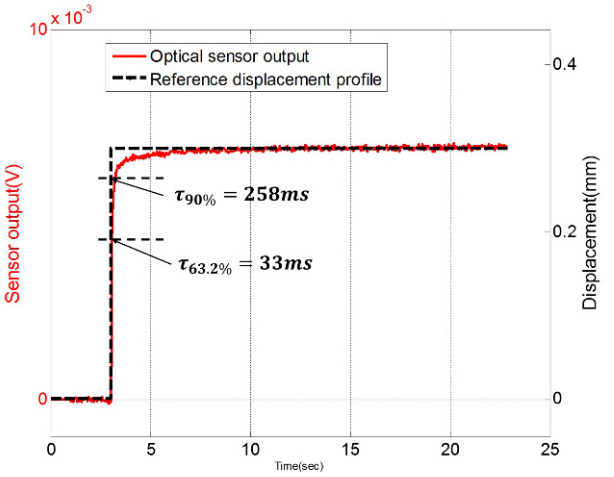

Fig. 7. Step response of the optical sensor and the displacement profile.

4.2. Dynamic test: sinusoidal loading

Fig. 8(a) shows the dynamic response of the proposed sensor during loading/unloading cycle with 0-6 N range in 0.5 Hz cycles. Our proposed sensor is highly linear to the reference force during loading phase. However, it shows nonlinearity during unloading phase since the sensor structure takes time to restore to its original shape. Fortunately, we aimed to use our proposed sensor as the force sensor to extract the human intention so the loading phase is more important than unloading phase. Fig. 8(b)

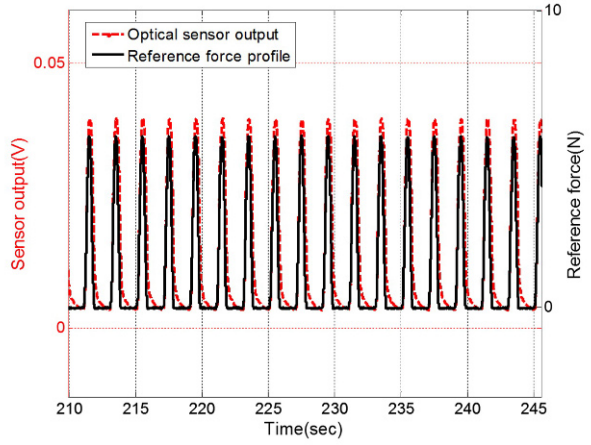

(a)

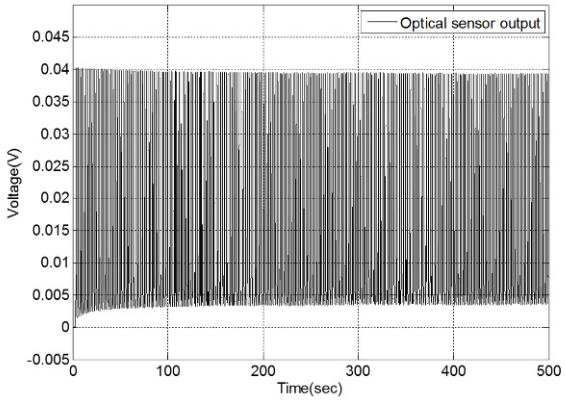

(b)

Fig. 8. (a) Sensor response during 15 cycles of loading/unloading (from 0 to 6N), (b) Long term reliability of optical sensor output.

represents that the proposed sensor demonstrates long-term stability followed by loading and unloading more than 200 cycles. The sensor responds to the cyclic loading with a good stability and reproducibility. We observed the baseline drift of the cyclic loading as 0.003 V, 9.5% of full scale. The reason of the baseline drift of the sensor voltage output is the effect of the residual strain in viscoelastic material [35]. The baseline drift gradually attenuates after several loadings. This result implies that the soft sensor shows better performance once pre-load or pre-strain are applied.

4.3. System identification: first order model approximation

To identify the relationship between force signal from load cell and sensor voltage output in loading phase, we set up the logic flow as shown in Fig. 9. The transfer function G_1 represents the proposed sensor response with respect to the displacement input from the test bed. In the same

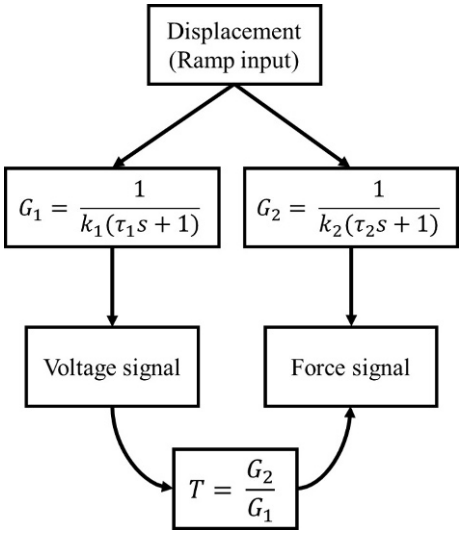

Fig. 9. The logic flow of system identification.

manner, G_2 represents that of the load cell response. After we get each of transfer functions, the relationship between the voltage to the force, the transfer function T, is derived as G_2/G_1. We assumed our sensor system to be a first order system, Kelvin-Voigt model, since it is one of the basic models representing viscoelastic material behavior. The model consists of two components, linear spring and damper, in parallel. The response of Kelvin-Voigt model is as follows:

$$\frac{x(output)}{F(input)} = \frac{1}{k(\tau s+1)} = \frac{C(s)}{R(s)}, \tag{1}$$

where τ is the time constant of the system, and $C(s)$ and $R(s)$ are the Laplace function for output and input, respectively. For a ramp input, $R(s)$ is given by

$$\mathrm{R}(s) = \frac{1}{S^2}. \tag{2}$$

Then, we can get the output, $C(s)$, in laplace domain as follows:

$$C(s) = \frac{1}{k} \cdot \frac{1}{S^2(\tau s+1)}. \tag{3}$$

By solving the equation through partial fraction, we can get the output, $C(t)$, in time domain.

$$C(t) = \frac{1}{k}\left(t - \tau\left(1 - e^{\left(-\frac{t}{\tau}\right)}\right)\right). \tag{4}$$

Fig. 10 shows the results of the system identification. We applied ramp displacement input with 1 mm/s for 0.5 seconds. In [36], the author suggests that the deformation should be less than 10% of the sample thickness. The material linearity is only maintained when the deformation is small, relative to the size of the sample. Referring to this information, we applied ramp deformation input which is

Table 2. k value, time constant and R^2 of each of output profiles and Transfer function T $(0.05-0.55$ sec).

Output	k	Time constant	R^2	Transfer function T
Voltage output	6.0005	0.4977	0.9995	$\frac{6.0005(0.4977s+1)}{0.0401(0.4880s+1)}$
Reference force	0.0401	0.4880	0.9997	≈ 150

around 20% of the thickness. The results are shown in Fig. 10(a) and (b). We observed that each of time constants, τ_1 and τ_2, was almost similar. Thus, these results show that the transfer function G_1 and G_2 are equivalent. The relationship between reference force and optical sensor voltage output voltage was linear and the slope was 150 as shown in Fig. 10(c) and Table 2. This is similar to the ratio between k_1 and k_2. This result explains the linear behavior of the reference force and sensor voltage output. The sensor voltage output behavior is mainly dependent on the deformation of viscoelastic structure. As long as a material linearity is preserved, we can approximate the sensor voltage output and the reference force as linear.

5. USER INTENTION EXTRACTION: FORCE ESTIMATION

As mentioned before, the contact force is used to extract the human intention in hand exoskeleton. The force estimated from the proposed sensor can be used in assistive force control [37]. The assistive force is propotional to the estimated force in the limited range. In this section, as a preliminary experiment, a force estimation test was executed. To validate the performance of the sensor, we integrated the sensor into the fabric glove. The target motion was a flexion motion of an index finger. To simulate the natural grip motion, cylindrical shape object combined with the load cell (FAY 333, KTOYO Co., Ltd., Uijeongbu, Korea) was used as a test bed as shown in Fig. 11(a). Two different surface shapes were tested, curved one and flat one. Fig. 11(b) show that the force estimation results in 10 cycles of the index finger flexion motion. The force range we tested was up to 5N. In the flat surface test, the root-mean-square error (RMSE) was 0.3018N with respect to the peak force 4.77 ($R^2 = 0.96$). For the curved surface test, RMSE was 0.2236N with respect to the peak force 4.54 N ($R^2 = 0.97$).

In order to investigate how the variation of contact point affects the sensor performance, we conducted the same test along with changing the angle between the finger and the surface of the load cell; 45, 60 degree. R-squared values of the 45 and 60 degree cases were 0.88 and 0.88 respectively (See Fig. 11(c)). We observed that the sensor performance attenuated as the amount of the angle increased. The accuracy of the sensor is maximized when

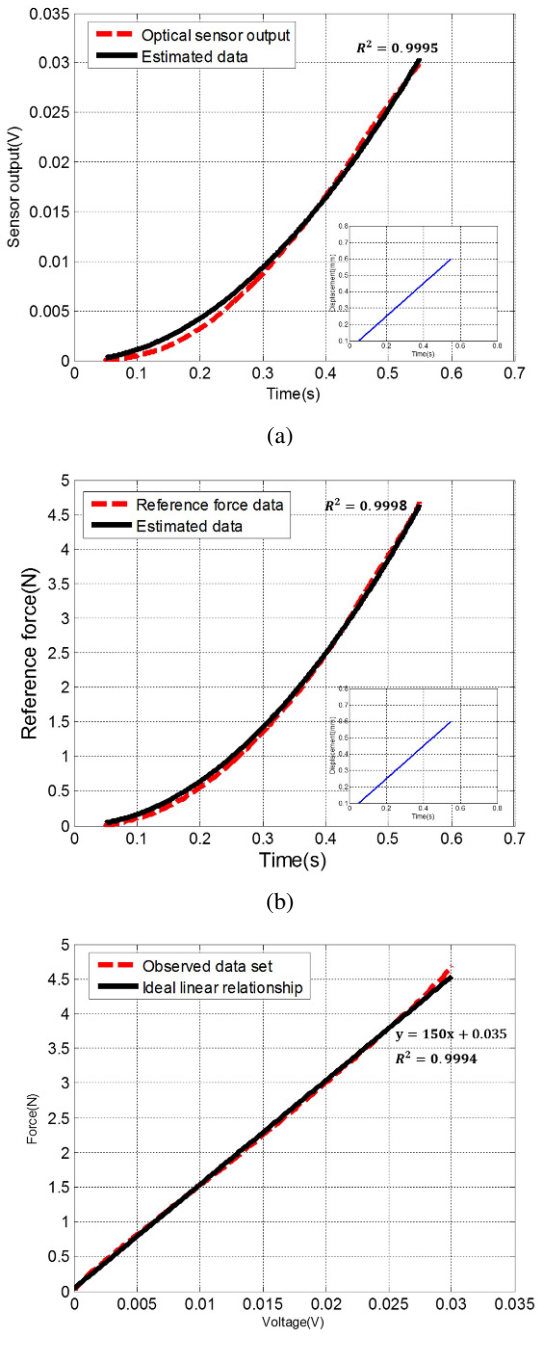

Fig. 10. Experimental data from (a) the optical sensor and (b) the reference force sensor and simulated results from Kelvin-Voigt model respectively (c) Reference force to optical sensor voltage output voltage curve.

the wearer applies the force in normal direction to objects. The most natural and stable position to grab an object lets the wearer to apply the finger force in perpendicular to the object. This is because we acquired the largest grip force when the finger applied the force in normal direc-

tion. Thus, we assumed the natural grip motion leads to the optimal case.

6. CONCLUSION

In this study, a design, development and characterization of a soft optical fingertip force sensor are presented. The design of the sensor is aimed for covering the distal phalange of finger, leaving the finger pad widely opened for tactile sensation. We executed the design parameter study from both perspectives: base/agent ratio and cross sectional shape. The lowest base/agent ratio (10:1) showed the good performance when it came to the sensor linearity ($R^2 = 0.9985$) and the lowest offset (6.09×10^{-5} V). However, the tradeoff was the sensitivity (0.0012 V/N) and the flexibility of the sensor, which is highly related to the wearibility. The proposed sensor showed fast response ($\tau = 33$ ms) in static test and high reliability and repeatability in sinusoidal loading and unloading. In the case of calibration, we applied the ramp input of displacement and then observed both reference force data and optical sensor voltage output. In the limited time duration, we observed the linear relationship between optical sensor voltage output and the reference force data.

These results imply that the signal from optical sensor and reference force data are linear as long as material linearity is maintained. Finally, we integrated the proposed sensor into the fabric glove to validate the performance. As a future work, we will derive the deformation model of the sensor based on the Hertz contact theory. Furthermore, force estimation experiments with various contact surfaces will be tested to analyze the robustness of the model and sensor system. Eventually, we will integrate the sensor into a hand assistive glove and validate the perfomance of the actuating system for patients.

REFERENCES

[1] A. A. Sayer, H. E. Syddall, H. J. Martin, E. M. Dennison, H. C. Roberts, and C. Cooper, "Is grip strength associated with health-related quality of life? Findings from the Hertfordshire Cohort Study," *Age Ageing*, vol. 35, no. 4, pp. 409-415, 2006. [click]

[2] S. Katz, A. B. Ford, R. W. Moskowitz, B. A. Jackson, and M. W. Jaffe, "Studies of Illness in the Aged," *J. Am. Med. Assoc. Med. Assoc.*, vol. 185, no. 12, pp. 914-919, 1963.

[3] H. Frederiksen, J. Hjelmborg, J. Mortensen, M. Mcgue, J. W. Vaupel, and K. Christensen, "Age Trajectories of Grip Strength: Cross-Sectional and Longitudinal Data Among 8,342 Danes Aged 46 to 102," *Ann. Epidemiol.*, vol. 16, no. 7, pp. 554-562, 2006. [click]

[4] E. J. Metter, R. Conwit, J. Tobin, and J. L. Fozard, "Age-associated loss of power and strength in the upper extremities in women and men," *J Gerontol A Biol Sci Med Sci*, vol. 52, no. 5, pp. B267-76, 1997.

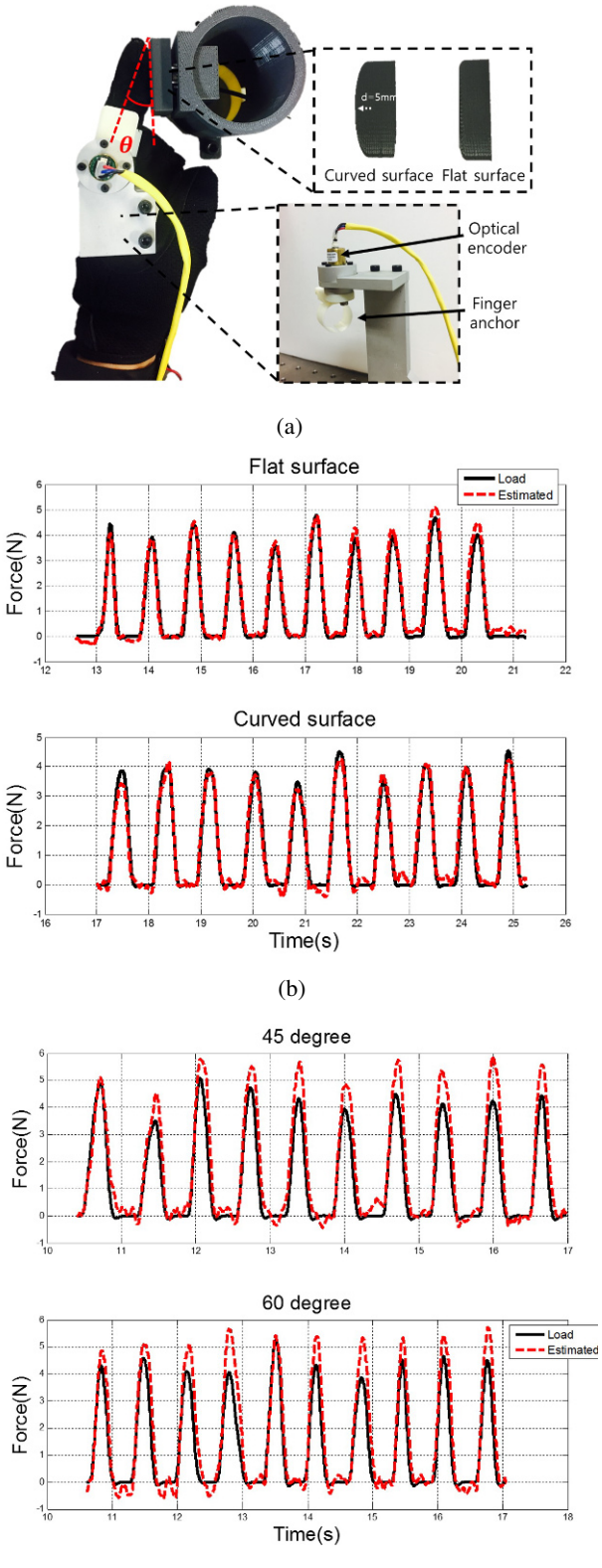

Fig. 11. (a) The force estimation test bed (b) The experiment result: Flat surface and Curved surface (c) The effects of the angle between the finger and the surface of the load cell.

[5] P. Helliwell, A. Howe, and V. Wright, "Functional assessment of the hand: reproducibility, acceptability, and utility of a new system for measuring strength.," *Ann. Rheum. Dis.*, vol. 46, no. 3, pp. 203-8, 1987.

[6] S. A. Sisto and T. Dyson-Hudson, "Dynamometry testing in spinal cord injury," *J. Rehabil. Res. Dev.*, vol. 44, no. 1, p. 123, 2007. [click]

[7] A. Sunderland, D. Tinson, L. Bradley, and R. Hewer, "Arm function after stroke. An evaluation of grip strength as a measure of recovery and a prognostic indicator," *J Neurol Neurosurg Psychiatry*, vol. 52, no. 11, p. 1267-, 1989.

[8] A. E. Barr, M. F. Barbe, S. Billing, B. D. Clark, S. Changes, and F. Email, "Work-Related Musculoskeletal Disorders?: Epidemiology, Pathophysiology, and Sensorimotor Changes," *Rev. Lit. Arts Am.*, vol. 34, no. 10, pp. 610-627, 1998.

[9] J. Ingvast and J. Wikander, "The Soft Extra Muscle system for improving the grasping capability in neurological rehabilitation," *Biomed. Eng. Sci. (IECBES), 2012 IEEE EMBS Conf.*, no. December, pp. 412-417, 2012.

[10]] M. A. Diftler, C. A. Ihrke, L. B. Bridgwater, D. R. Davis, D. M. Linn, E. A. Laske, K. G. Ensley, and J. H. Lee, "RoboGlove-A robonaut derived multipurpose assistive device," *Proc. of Int. Conf. Robot. Autom.*, 2014.

[11] M. D. Baker, K. Mcdonough, E. M. Mcmullin, M. Swift, and B. F. Busha, "Orthotic hand-assistive exoskeleton," *Bioeng. Conf. (NEBEC), 2011 IEEE 37th Annu*. Northeast, pp. 3-4, 2011.

[12] Y. Yamada, T. Morizono, S. Sato, T. Shimohira, Y. Umetani, T. Yoshida, and S. Aoki, "Proposal of a SkilMate finger for EVA gloves," *Proc. of IEEE Int. Conf. Robot. Autom.*, vol. 2, pp. 1406-1412, 2001.

[13] M. Takagi, K. Iwata, Y. Takahashi, S. I. Yamamoto, H. Koyama, and T. Komeda, "Development of a grip aid system using air cylinders," *Proc. - IEEE Int. Conf. Robot. Autom.*, pp. 2312-2317, 2009.

[14] K. Toya, T. Miyagawa, and Y. Kubota, "Power-Assist Glove Operated by Predicting the Grasping Mode," *J. Syst. Des. Dyn.*, vol. 5, no. 1, pp. 94-108, 2011.

[15] N. Benjuya and S. B. Kenney, "Myoelectric Hand Orthosis," *JPO Journal of Prosthetics & Orthotics*, vol. 2. Journal of Prosthetics and Orthotics, pp. 149-154, 1990.

[16] L. Lucas, M. Dicicco, and Y. Matsuoka, "An EMG-Controlled Hand Exoskeleton for Natural Pinching," *J. Robot. Mechatronics*, vol. 16, no. 5, pp. 1-7, 2004.

[17] D. A. Nowak, J. Hermsdörfer, S. Glasauer, J. Philipp, L. Meyer, and N. Mai, "The effects of digital anaesthesia on predictive grip force adjustments during vertical movements of a grasped object," *Eur. J. Neurosci.*, vol. 14, no. 4, pp. 756-762, 2002.

[18] M. Nakatani, T. Kawasoe, K. Shiojima, K. Koketsu, S. Kinoshita, and J. Wada, "Wearable contact force sensor system based on fingerpad deformation," *Proc. of IEEE World Haptics Conf. WHC 2011*, pp. 323-328, 2011.

[19] P. Heo, S. J. Kim, and J. Kim, "Powered finger exoskeleton having partially open fingerpad for flexion force assistance," *Proc. of IEEE/ASME Int. Conf. Adv. Intell. Mechatronics Mechatronics Hum. Wellbeing, AIM 2013*, vol. 2, pp. 182-187, 2013.

[20] S. A. Mascaro and H. H. Asada, "Measurement of finger posture and three-axis fingertip touch force using fingernail sensors," *IEEE Trans. Robot. Autom.*, vol. 20, no. 1, pp. 26-35, 2004.

[21] D. Vogt, Y. Menguc, Y. Park, and M. Wehner, "Progress in Soft, Flexible, and Stretchable Sensing Systems," *Biorobotics.Harvard.Edu*, pp. 0-1, 2013.

[22] D. M. Vogt, Y.-L. Park, and R. J. Wood, "Design and Characterization of a Soft Multi-Axis Force Sensor Using Embedded Microfluidic Channels," *IEEE Sens. J.*, vol. 13, no. 10, pp. 4056-4064, 2013.

[23] J. Chossat, Y. Tao, V. Duchaine, and Y. Park, "Wearable Soft Artificial Skin for Hand Motion Detection with Embedded Microfluidic Strain Sensing," *Proc. of IEEE Int. Conf. Robot. Autom.*, pp. 2568-2573, 2015.

[24] Y. Menguc, Y. L. Park, E. Martinez-Villalpando, P. Aubin, M. Zisook, L. Stirling, R. J. Wood, and C. J. Walsh, "Soft Wearable Motion Sensing Suit for Lower Limb," *Proc. of IEEE Int. Conf. Robot. Autom. (ICRA)*, pp. 5289-5296, 2013.

[25] M. Amjadi, A. Pichitpajongkit, S. Lee, S. Ryu, and I. Park, "Highly stretchable and sensitive strain sensor based on silver nanowire-elastomer nanocomposite," *ACS Nano*, vol. 8, no. 5, pp. 5154-5163, 2014. [click]

[26] M. Amjadi, Y. J. Yoon, and I. Park, "Ultra-stretchable and skin-mountable strain sensors using carbon nanotubes-Ecoflex nanocomposites.," *Nanotechnology*, vol. 26, no. 37, p. 375501, 2015. [click]

[27] A. V. Shirinov and W. K. Schomburg, "Pressure sensor from a PVDF film," *Sensors Actuators, A Phys.*, vol. 142, no. 1, pp. 48-55, 2008.

[28] M. Acer, M. Salerno, K. Agbeviade, and J. Paik, "Development and characterization of silicone embedded distributed piezoelectric sensors for contact detection," *Smart Mater. Struct.*, vol. 24, no. 7, p. 75030, 2015.

[29] D. Kwon, T. Lee, J. Shim, S. Ryu, M. Kim, S. Kim, T. Kim, and I. Park, "Highly Sensitive, Flexible, and Wearable Pressure Sensor Based on a Giant Piezocapacitive Effect of Three-Dimensional Microporous Elastomeric Dielectric Layer," *ACS Appl. Mater. Interfaces*, vol. 8, no. 26, pp. 16922-16931, 2016. [click]

[30] M. Ramuz, B. C. K. Tee, J. B. H. Tok, and Z. Bao, "Transparent, optical, pressure-sensitive artificial skin for large-area stretchable electronics," *Adv. Mater.*, vol. 24, no. 24, pp. 3223-3227, 2012. [click]

[31] S. Yun et al., "Polymer-waveguide-based flexible tactile sensor array for dynamic response," *Adv. Mater.*, vol. 26, no. 26, pp. 4474-4480, 2014. [click]

[32] C. To, T. L. Hellebrekers, and Y. L. Park, "Highly stretchable optical sensors for pressure, strain, and curvature measurement," *IEEE Int. Conf. Intell. Robot. Syst.*, vol. 2015-Decem, pp. 5898-5903, 2015.

[33] B. Lee, "Review of the present status of optical fiber sensors," *Opt. Fiber Technol.*, vol. 9, no. 2, pp. 57-79, 2003. [click]

[34] D. A. Chang-Yen, R. K. Eich, and B. K. Gale, "A monolithic PDMS waveguide system fabricated using soft-lithography techniques," *J. Light. Technol.*, vol. 23, no. 6, pp. 2088-2093, 2005.

[35] E. Tanaka, M. Tanaka, J. Aoyama, M. Watanabe, Y. Hattori, D. Asai, T. Iwabe, A. Sasaki, M. Sugiyama, and K. Tanne, "Viscoelastic properties and residual strain in a tensile creep test on bovine temporomandibular articular discs," *Arch. Oral Biol.*, vol. 47, no. 2, pp. 139-146, 2002. [click]

[36] B. Qiang, J. Greenleaf, M. Oyen, and X. Zhang, "Estimating material elasticity by spherical indentation load-relaxation tests on viscoelastic samples of finite thickness," *IEEE Trans. Ultrason. Ferroelectr. Freq. Control*, vol. 58, no. 7, pp. 1418-1429, 2011.

[37] P. Heo and J. Kim, "Power-assistive finger exoskeleton with a palmar opening at the fingerpad," *IEEE Trans. Biomed. Eng.*, vol. 61, no. 11, pp. 2688-2697, 2014.

Haedo Cho received the M.S. degree from the Department of Mechanical engineering, Korea Advanced Institute of Science and Technology, Daejeon, Korea, in 2016. His research interests include soft tactile sensors and power assistive devices.

Hyosang Lee received the M.S. degree from Korea Advanced Institute of Science and Technology, Daejeon, Korea, in 2012, where he is currently pursuing the Ph.D. degree, both in mechanical engineering. His research interests include artificial tactile skin, nanocomposites, signal processing.

Yeongjin Kim is currently an Assistance Professor in the Department of Mechanical Engineering at Incheon National University. He received his B.A, M.A. and Ph.D. in Mechanical Engineering, in 2006, 2008 and 2012, respectively, all from the Korea Advance Institute of Science and Technology. He was also a Research Associate in the Department of Mechanical Engineering at University of Maryland, College Park (UMCP). His research interests are primarily in the area of MR-compatible surgical robotics, rehabilitation robotics, grasping, and mechanical cancer diagnosis.

Jung Kim received the Ph.D. degree from the Department of Mechanical Engineering, Massachusetts Institute of Technology, Cambridge, MA, USA. He is currently a Professor in the Department of Mechanical Engineering, Korea Advanced Institute of Science and Technology, Daejeon, Korea. His current research interests include haptics, biosignal analysis for healthcare, and physical human–robot interactions.